Desalination and Water Treatment
www.deswater.com

doi: 10.5004/dwt.2023.29193

283 (2023) 36–49
January

Removal of Cr(III) from tannery wastewater using *Citrus aurantium* (grapefruit peel) as biosorbent

Zaida Rabago-Velasquez[a], Laura Patiño-Saldivar[a], Alba N. Ardila A.[b], Alfonso Talavera-Lopez[c], Mercedes Salazar-Hernández[d], Rosa Hernández-Soto[a], José A. Hernández[a,*]

[a]*UPIIG, del Instituto Politécnico Nacional. Av. Mineral de Valencia No. 200, Col. Fracc. Industrial Puerto Interior, Silao de la Victoria, Guanajuato, México, CP. 36275, emails: jahernandezma@ipn.mx (J.A. Hernández), zrabagov1601@alumno.ipn.mx (Z. Rabago-Velasquez), patinio2103@gmail.com (L. Patiño-Saldivar), rohernandezs@ipn.mx (R. Hernández-Soto)*
[b]*Politécnico Colombiano Jaime Isaza Cadavid, carrera 48 No. 7–151, Medellín, Colombia, CP 4932, email: anardila@elpoli.edu.co*
[c]*Unidad de Ciencias Químicas, Universidad de Zacatecas, Campus UAZ siglo XXI, Carretera a Guadalajara km 6, ejido la escondida, Zacatecas, CP. 98160, México, email: talavera@uaz.edu.mx*
[d]*Departamento de Ingeniería en Minas, Metalurgia y Geología, División de Ingenierías, Universidad de Guanajuato 3600, México, email: merce@ugto.mx*

Received 2 June 2022; Accepted 10 December 2022

ABSTRACT

Tanneries that use Cr(III) in their processes are among the industries that can cause environmental contamination by this heavy metal. Therefore, the use of grapefruit peel (GP) as a novel biosorbent for removal was investigated Cr(III) GP was treated with water grapefruit peel (WGP) and methanol grapefruit peel (MGP), considering parameters such as pH, contact time and initial concentration of Cr and evaluating their effect on biosorption. The adsorption capacity at a pH of 2.74 for WGP and MGP achieved 85.75% and 96.60%, respectively. Freundlich model indicated an adsorption favorable heterogeneous chemical process. The kinetic study indicated that Cr removal is due to simultaneous physicochemical processes. The analysis of attenuated total reflectance-Fourier-transform infrared spectroscopy showed the presence of pectin, lignin and cellulose that helps adsorption due to the participation of their functional groups. X-ray diffraction and scanning electron microscopy-energy-dispersive X-ray spectroscopy analysis found that the adsorption of Cr on the surface caused significant changes in the network parameter, which confirmed that there is an ions substitution between Ca and Cr at the biosorbent surface.

Keywords: Biosorption; Ion-exchange; Removal of chromium; Removal of metals; Bioadsorbent

1. Introduction

Industrial processes generate a vast abundance of waste involving organic and inorganic contaminants that contaminate surface and groundwater when not adequately treated [1–3]. Water contamination directly humans, flora and fauna, so it is essential to remove such contaminants before effluents are discharged into the environment [1–4]. The largest source of these wastes are residues from pesticide paints, coal conversion, mining, fertilizers, tanning, alloys, polymeric resins, dyes, explosives, insecticides, the oil industry, foundry and petrochemicals, domestic

* Corresponding author.

activities, and agriculture. These anthropogenic activities have accelerated the accumulation and bioavailability of these harmful compounds in the biosphere [3–6]. Several conventional technologies (physio and chemical) have been used to eliminate compounds in aqueous solutions, which have advantages and disadvantages such as high operating costs, energy consumption and regeneration, low selectivity and efficiency, and generation of secondary pollutants [7,8]. These conventional methods include ion exchange, solvent extraction, coagulation, chemical precipitation and reduction, membrane filtration, electrodeposition, reverse osmosis, and adsorption [7,9]. The latter is one of the most effective for the removal of compounds from water using natural materials, resins, and activated carbon obtained from different sources as common adsorbents among others [10–12].

The use of dead or live biomass to remove contaminants is known as biosorption, which has its main advantages as low operating cost, easy handling, versatility, better selectivity, effectiveness, and, most interesting of all, not producing secondary contaminants that can be toxic [13–15]. Therefore, the valuation and reuse of these low-cost natural by-products to remove pollutants is an attractive practice seeking a positive way to contribute to the local environment and decrease the environmental impact of industrial activities [12–16,17]. The biosorbents used for metal ions removal can be classified as bacteria, fungi, algae, industrial and agricultural waste [17–21]. Waste from the food and juice industry, especially fruit and vegetable peels, is generated in large quantities from which a wide availability of biodegradable biosorbents can be obtained [16,22,23]. Moreover, these potential biosorbents can be even more interesting from the environmental point of view when subjected to easy pretreatments to improve their adsorption capacity [6,16,23]. Four million tons of grapefruit are produced worldwide. From this weight, 44%–55% is peel discharged as garbage every year (about 1.7 tons). Moreover, the incorrect disposal of such solid wastes can cause water contamination due to their soluble and insoluble monomers and polymers [7,24,25].

Grapefruit peel (GP) soluble parts contain glucose, fructose, sucrose, and xylose, while the insoluble parts have pectin, cellulose, hemicellulose and lignin which are rich in carboxylic and hydroxyl groups [10,26]. GP has already been used as a biosorbent for the removal of dyes such as methylene blue [3] and crystal violet [27], among others [8,16], and heavy metal ions such as Ni, Cd, Zn, Cu, Cr(VI), lanthanides [2,28], having a removal percentage of 80% to 99% and an adsorption capacity between 14 and 88 m/g for various heavy metals such as Ar, Cd, Cr(VI), Pb, Zn mainly, used different methods of modification of the GP surface using acids as solvents (citric, sulfuric, hydrochloric, among others [28,29]. In addition, GP has been treated with methanol mainly to obtain various compounds (polyphenols, flavonoids, etc.) that are used in different industries such as food, pharmaceuticals, among others. After this process treated GP is discarded, however, there is an opportunity to use this biomass as a biosorbent to finally have a process train where added value compounds and a material can to remove contaminants from aqueous solutions such as Cr(III). Chromium is widely used in various industries where its waste is a major environmental problem because these effluents have a Cr(III) concentration between 200 and 2,000 mg/L with a pH less than 3.5 and are usually toxic at these concentrations to both For aquatic life, as for human life [19,30–33]. The situation requires removing Cr(III) from these effluents before they are discharged into the drainage. For this reason, in this study the adsorption capacity of GP treated with methanol and water was analyzed using aqueous solutions of Cr(III) at a pH lower than 3.5, trying to simulate the real conditions of the effluents of the tanneries and analyzing the surface of the biomaterial to know the elimination mechanism, as well as the influence of pH, contact time, initial concentration of Cr(III) Ions and biosorbent concentration together with the interaction of the functional groups present on the GP surface treated in the process of adsorption.

2. Materials and methods

2.1. Reagents

All reagents used were analytical grade. Deionized water was used to prepare test solutions at 0–1,000 mg/L concentrations. In addition, the company Cuero Centro, S.A. of C.V. donated chromium salt ($2Cr(OH)SO_4 \cdot xNa_2SO_4$) used in the tanning process.

2.2. Pretreatment of grapefruit peel

The grapefruit peel (*Citrus aurantium*) was collected and washed Then GP was dried at a temperature of 90°C for 2 d and crushed until a particle size of 0.3 mm was obtained using sieving equipment (WACO-TYLER RX-29). Subsequently, 50% (wt/v) of grapefruit peel was treated at 120°C (water) and 35°C (methanol) orbital stirring. Finally, samples were filtered and dried at 60°C in a forced convection oven (Shel Lab CE5F) for 24 h. In methanol grapefruit peel (MGP), the shell-solvent mixture was left 72 h at 200 rpm at 35°C in a shaker (ZICHENG ZHWY-200D). This procedure was repeated seven times, while water grapefruit peel (WGP) was carried out at 80°C for 1 h with vigorous stirring. This procedure was done until the filtrate no longer showed any color in the wastewater [24]. Finally, the resulting GP was stored in an airtight bottle at ambient temperature until use.

2.3. Cr(III) adsorption isotherms with GP

For the equilibrium studies of Cr(III) adsorption in WGP and MGP 0.5 g were set in contact with 25 mL of Cr(III) solution (ZICHENG ZHWY-200D) an orbital shaking at 200 rpm at 30°C for 24 h. The Cr(III) concentration in this experiment ranged from 0 to 1,000 mg/L, with pH of 0.93, 1.76 and 2.74. After sample aliquots were taken, centrifuged (Generic 6-TRPR) at 4,000 rpm for 10 min and subsequently the absorbance was measured in the UV-Vis spectrum (Velab VE-5000) at 425 nm to determine the residual concentration of Cr(III) [29,34,35]. The adsorption capacity (q) of Cr(III) was determined with Eq. (1) [36–38]:

$$q_e = \frac{\left(C_0 - C_e\right)V}{m} \tag{1}$$

where C_o and C_e correspond to the initial and equilibrium concentration (mg/L), respectively, V is the volume of solution (L) and m is the mass of the adsorbent (g). The most used non-linear adsorption isotherm models are shown in Table 1.

In the Dubinin–Radushkevich isotherm the mean energy of sorption, E, is calculated by Eq. (2) [5,40]:

$$E = \frac{1}{\sqrt{2k_{DR}}} \tag{2}$$

The magnitude of E helps estimate the type of biosorption reaction. Another parameter that was determined, with the help of Eq. (3), was the removal percentage, $\%R_{Cr}$, [31,40]:

$$\%R_{Cr} = \frac{(C_0 - C)}{C_0} \times 100 \tag{3}$$

The Gibbs free energy (ΔG) was calculated by using Eq. (4) [36,41]:

$$\Delta G = -RT \ln\ln(55.5K_L) \tag{4}$$

where K_L is the Langmuir model constant (L/mol), R is the ideal gases constant (kJ/mol·K) and T is the absolute temperature (K). The separation factor, R_L, was calculated using Eq. (5) [31]:

$$R_L = \frac{1}{1 + K_L C_0} \tag{5}$$

From the proposed models it has to be chosen which one fits the best, for this, two different criteria were used: the first of them was the deterministic coefficient (R^2) which must have a value close to 1 to consider a possible adjustment, the second criterion is the normalized coefficient of determination, Δq, which was determined with the help of Eq. (6) [24,31]:

Table 1
Non-linear adsorption isotherm models [18,38,39]

Model	Equation
Langmuir	$q_e = \frac{q_m K_L C_e}{1 + K_L C_e}$
Temkin	$q_e = A + B\ln(C_e)$
Freundlich	$q_e = K_F C_e^{1/n}$
Dubinin–Radushkevich (DR)	$q_e = q_m \exp(-k_{DR}\varepsilon^2)$
Sips	$q_e = \frac{q_m (K_s C_e)^{n_s}}{1 + (K_s C_e)^{n_s}}$
Redlich–Peterson (RP)	$q_e = \frac{K_R C_e}{1 + a_R C_e^{n_{RP}}}$

$$\Delta q = \sqrt{\frac{\left(\frac{q_{exp} - q_{cal}}{q_{exp}}\right)^2}{N-1}} \times 100 \tag{6}$$

where N is the number of data, q_{exp} and q_{cal} (mg/g) are the values of the experimental adsorption capacity and calculated by the model, respectively.

2.4. Cr(III) batch adsorption kinetics

The kinetics of Cr(III) biosorption was carried out to investigate the evolution of Cr(III) adsorption in the bioadsorbent. The mass of GP varied from 0.1 to 0.5 g with 50 mL of Cr(III) solution at 600 mg/L at pH 0.93, 1.76 and 2.74. Samples were placed in closed containers in a shaker (ZICHENG ZHWY-200D) at 200 rpm and at 30°C. Aliquots were taken every 1.5 h to separate the biosorbent by centrifugation (Generic 6-TRPR) at 4,000 rpm and the supernatant liquid was analyzed to determine the concentration of the different ions present in the solution [31]. Table 2 concentrates on the different kinetic models of Cr(III) biosorption.

2.5. GP characterization before and after biosorption

Attenuated total reflectance-Fourier-transform infrared spectroscopy (ATR-FTIR) was used to analyze the biosorbent before and after adsorption. The infrared spectrum was analyzed wave number ranging from 4,000–400 cm^{-1} using a Thermo Scientific Nicolet iS10 analyzer. In total, 32 scans were obtained with a resolution of 4 cm^{-1}. In addition, X-ray diffraction patterns (XRD) were obtained in a diffractometer (Ultima IV Rigaku) measuring from 4° to 80° in 2θ, using a step of 0.03°. To determine the isoelectric point was carried out using the mass titration method described by Hernandez-Maldonado et al. [32]: a sample of adsorbent in water with an initial ratio of 0.05 g was stirred at 200 rpm for 24 h. in 50 mL to determine its pH with a potentiometer (Science Med SM-25CW), 0.05 g was added every 24 h until the pH did not change. The scanning electron microscopy images and the energy-dispersive X-ray spectroscopy (SEM-EDS-EDX) were obtained in a JOEL spectrometer (6510 pus).

3. Results and discussion

3.1. Parameters that affect the adsorption process

The equilibrium adsorption is a dynamic process influenced by many parameters such as the nature of the active sites on the biosorbent surface, limitations due to mass transfer, attraction–repulsion forces, and changes in the solubility of the solution due to a heterogeneous system.

3.1.1. Effect of the pH on adsorption of Cr(III)

The behavior of heavy metal ions and the active site charges in the biosorption are directly related to the pH. This parameter affects the solubility and ionization of metals and the electrostatic interaction [3,15,26,39–43]. In Fig. 1a the adsorption capacity increases as pH rises.

Table 2
Adsorption kinetic models are used to analyze experimental data [31,41,42]

Model	Equation	
Pseudo-first-order	$q = q_{max}\left[1-\exp\left(-k_1 t\right)\right]$	q_t is the adsorption capacity (mg/g); C_o is the initial concentration of the dye in the liquid (mg/L); V (L) is the volume of the dye solution; m (g) is the mass of the adsorbent.
Pseudo-second-order	$q = \frac{t}{\frac{1}{k_2 \times q_{max}^2} + \frac{t}{q_{max}}}$	q_{max} is the maximum adsorbed capacity (mg/g); k_1 (1/h) is the speed constant of the pseudo-first-order model;k_2 (g·s/mg) is the speed constant of the pseudo-second-order model.
Elovich	$q = \frac{1}{\beta}\left[\ln\left(t\right) + \ln\left(\alpha \times \beta\right)\right]$	k_{ID} (mg/g·h) is the speed constant of the intraparticle diffusion model.
Intraparticle diffusion	$q = k_{ID} t^{0.5}$	k_{ext} (1/h) is the speed constant of the model external diffusion.
External diffusion	$q = \frac{C_0 \cdot V}{m}\left[1-\exp\left(-k_{ext} \times t\right)\right]$	α is the initial rate of adsorption (mg/g·h); β is the constant of the Elovich model related to the surface area covered and the activation energy by chemisorption (mg/g).
Avrami	$q = q_{max}\left[1-\exp\left(-k_{A \times t}\right)^{n_A}\right]$	k_A kinetic constant (t^{-n}); n_A Avrami of exponent.

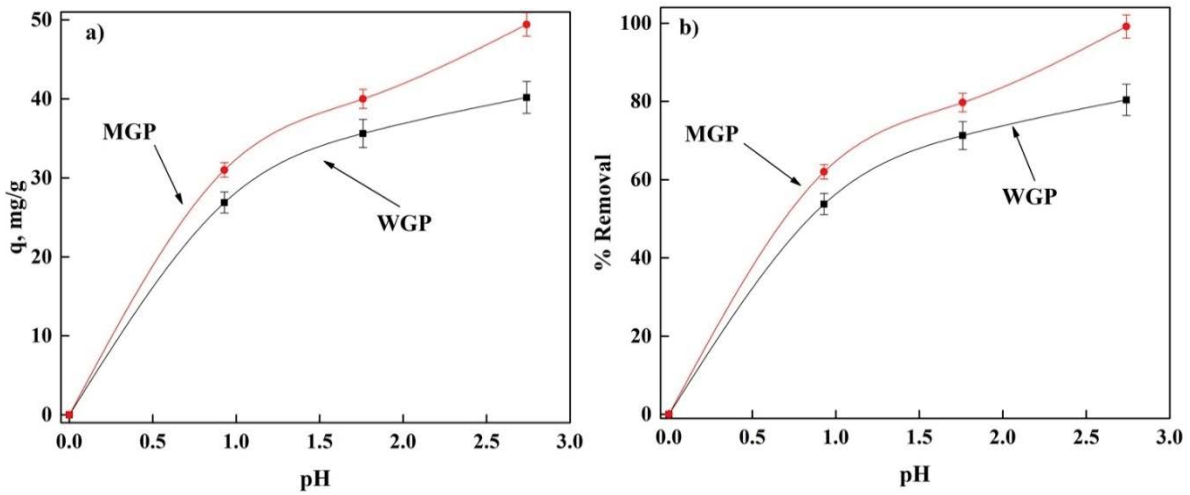

Fig. 1. pH influence during Cr(III) adsorption using GP biosorbents treated with water (WGP) and methanol (MGP). Temperature of 30°C, C_{ads} = 1 g/L and initial concentration of Cr(III) = 1,000 mg/L.

However, in the treatment with water it was observed that behavior tends to stabilize the adsorption capacity of Cr(III) at 41 mg/g while in the MGP there is a tendency to increase Cr(III) adsorption (>50 mg/g). This behavior was also observed with the removal percentage (1b) where there is 80% removal of Cr(III) for WGP and >99% removal for MGP. These results show the influence of the changes in surface of biosorbents moving from a positive charge to a negative charge favoring the transfer of ions between the solution and the active sites on the biosorbents surface [22,29,32,36,42–47]. The isoelectric point of biosorbent (pH_{pzc} = 5.75 and pH_{pzc} = 3.44 for WGP and MGP, respectively) indicates a protonic surface of the biosorbents, which explains removal percentage of approximately 100% for the treatment with methanol compared to the treatment with water (around 80%). These results also show differences between surface functional groups and active sites (Fig. 1b). In the particular case of GP treated with water, it has been reported that there is a linear increase in the percentage of removal from a pH of 2–5, with maximum removal of 55% due to the transition of the surface charge from positive to negative [3], This result obtained is lower than the one achieved in this work (82% removal) because the greatest amount of monomers and polymers soluble in GP were removed. On the other hand, Zhang et al. [43] reported that using biochar from chestnut shells, percent removal between 3.37% and 80.5% at a pH of 2 is achieved, also showing that high adsorption can be achieved even at a pH below one value of 3 because electrostatic forces are not the ones that govern the adsorption process, but other forces intervene.

3.1.2. Effect of initial Cr(III) concentration of adsorption

Mass transfer is part of the adsorption processes therefore, it is necessary to consider the effect of the initial

contaminant concentration as an important parameter [43]. Fig. 2 shows an increase in the removal efficiency of Cr(III) in GP for both pretreatments, noting a maximum removal of Cr(III) of 80% and 100%, for WGP and MGP. This result is achieved due to the number of surface sites capturing Cr ions [44]. This trend was reported for Cr(III) removal using other biosorbents [4,23,48,49]; however, other studies indicate that indicates the increase in the initial concentration decreases the efficiency of the biosorbent [3,49,50]. This disagreement may be due to the pretreatment and material selected for the adsorption process, as this directly affects the nature of the biosorbent surface.

3.1.3. Effect of adsorbent doses on Cr(III) adsorption

In this work, adsorbent doses ranged from 2 to 10 g/L with 600 mg/L as the initial Cr(III) concentration. Fig. 3 shows increased Cr(III) removal with a decrease in adsorption capacity as adsorbent doses rise from 2 to 10 g/L. With this increase in the mass of the biosorbent, there was a significant increase in the biosorption efficiency of 61.4% and 54.4% for a pH of 0.93 and 1.76, respectively, using WGP. In the case of MGP, a similar behavior was observed, having an increase in the removal of 71.4% and 40% for a pH of 0.93 and 1.76, respectively, with the increase in the concentration of the biosorbent. A pH of 2.7 was noted for both biosorbents, where the adsorption doses remain practically constant ($C_{ads} \geq 4$ g/L). This result may be because the external mass transfer in the adsorption process is negligible [23] allowing an exchange of Cr(III) ions from the solution towards the GP surface in a dynamic way, achieving equilibrium. However, at $C_{ads} < 4$ g/L there is a decrease in the adsorption percentage of 8.9% and 11% for WGP and MGP, respectively. The adsorption capacity decreases from 28% to 63.3% for a pH value of 0.93 and 1.74, respectively for WGP, and MGP there is a decrease in its adsorption capacity from 50% to 70% for a pH of 0.93 and 1.74, respectively. In the case of WGP and MGP at a pH of 2.7, there is a loss of adsorption capacity of around 85% with the increase in the concentration of the biosorbent. Therefore, these results, it can be mentioned that the optimal value of the biosorbent mass was 2 g/L.

This trend is like that obtained in various adsorbents with different contaminants [4,47,51]. When comparing the % of Cr(III) removal with adsorbent doses, our findings are within the range reported in the literature, mainly for PGM [4,15,26,48]. The adsorption process is considered a dynamic process, which allows the exchange of ions in the solution with the surface of the adsorbent, which, by increasing its presence in biosorption, has a greater surface area [15,42,49,51–56] allowing to increase the number of sites available for the elimination of metal ions increasing the removal [13,26,29], however, this results in a decrease in the adsorption capacity since the ions available to be adsorbed are insufficient to cover the active sites on the surface as the concentration of the adsorbent increases [15,21,29, 36,55].

3.2. Equilibrium of Cr(III) adsorption on WGP and MGP

The compression of the interaction between the Cr(III) ions and GP is analyzed by adjusting the experimental (Fig. 4) data with the different equilibrium models described in Table 3. The R^2 values are very similar also the normalized standard deviation ($\Delta q\%$) suggests that regardless of the pretreatment pH Freundlich best fits, that is, there are no limitations on the biosorbent surface with the formation of a multilayer (Table 3). As $n < 1$, $1/n > 1$ and $0 > R_L > 1$, adsorption process is favorable in all cases. Maximum adsorption at pH 0.93, 1.76 and 2.74 for WGP were 20.89, 35.63 and 41.12 mg/g, respectively. In addition, there was an increase in Cr(III) removal from 62% to 80.3% with a pH rise. Concerning MGP, the maximum adsorption capacity were 31, 39.85 and 49.43 mg/g at a pH of 0.93, 1.76 and 2.74, respectively, resulting in an increase in Cr(III) removal percentage from 65% to 99.9% with the increased pH, the increase in the values of q_{max} and K_L with the increase of temperature indicates that the biosorption process is endothermic thus having the same behavior reported in other studies where metal ions are removed [36].

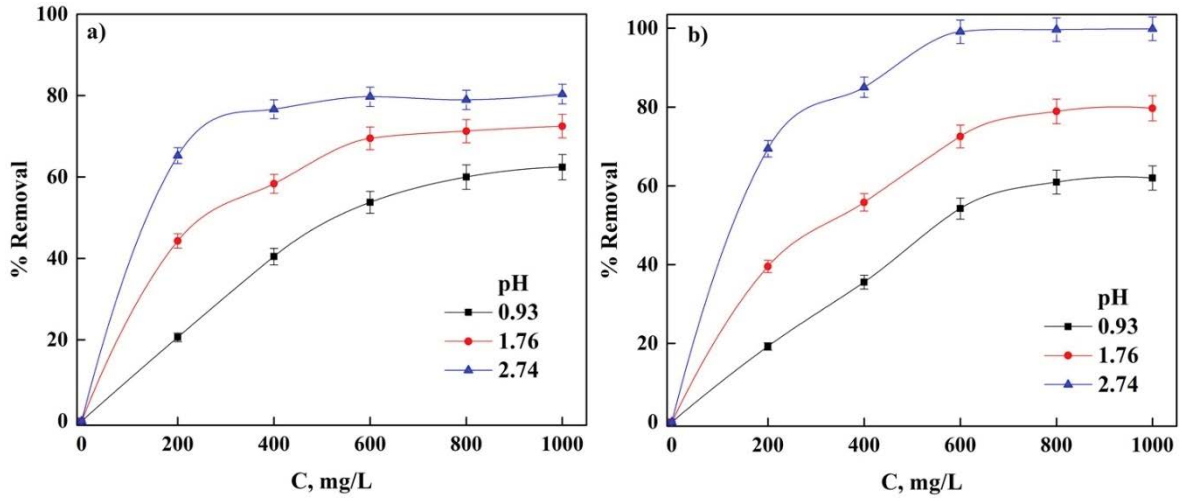

Fig. 2. Effect of the initial concentration on the biosorption of Cr(III) using GP biosorbents: (a) WGP and (b) MGP. Temperature of 30°C, C_{ads} = 1 g/L and initial concentration of Cr(III) = 0–1,000 mg/L.

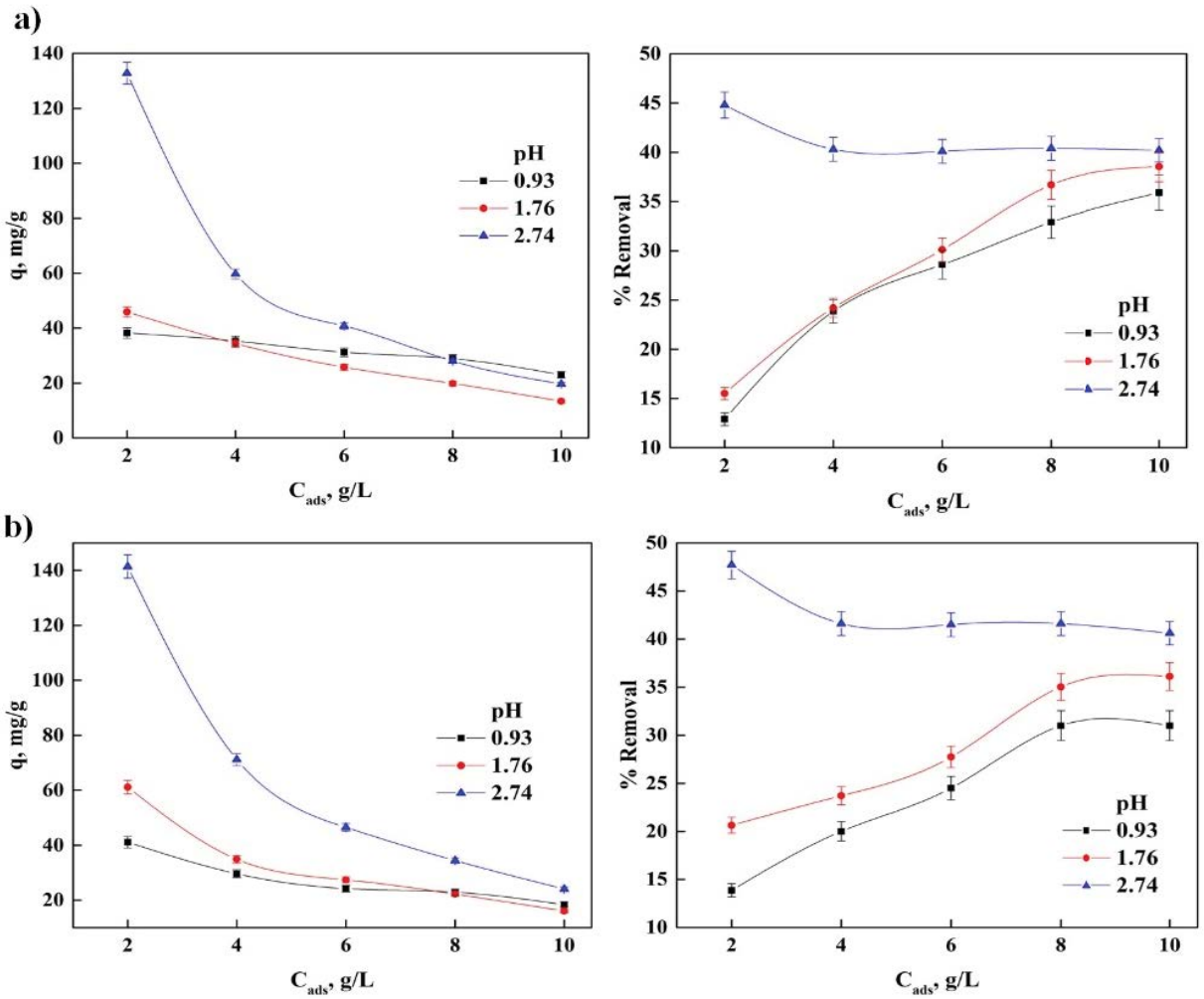

Fig. 3. Variations on adsorption capacity and Cr(III) removal percentage due to pH of the medium: (a) WGP and (b) MGP. Initial concentration of Cr(III) = 600 mg/L, temperature = 30°C and C_{ads} of 2 to 10 g/L.

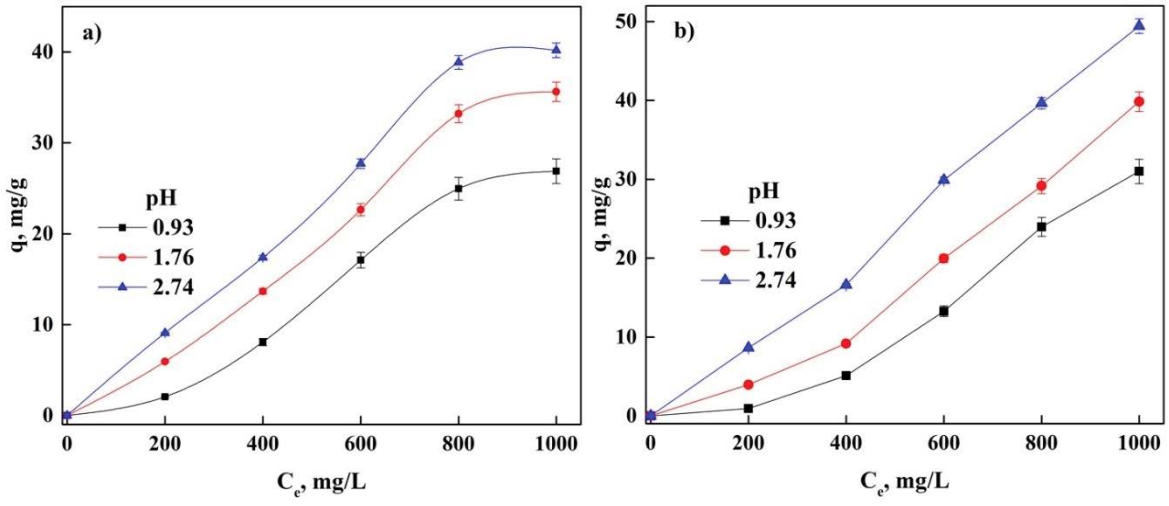

Fig. 4. Experimental data of Cr(III) adsorption at equilibrium, (a) WGP and (b) MGP. Temperature = 30°C, Cr(III) concentration = 0 to 1,000 mg/L and C_{ads} = 1 g/L.

Table 3
Parameters of the isotherm models for WGP and MGP

Model	Parameter	WGP			MGP		
		0.93	1.76	2.74	0.93	1.76	2.74
Langmuir	K_L, L/mg	0.0026	0.0031	0.0034	0.0017	0.0019	0.0025
	q_m, mg/g	27.01	36.02	41.05	32.05	40.51	50.01
	R_L	0.66–0.27	0.63–0.25	0.59–0.23	0.75–0.37	0.73–0.35	0.66–0.29
	R^2	0.723	0.783	0.813	0.670	0.731	0.798
	Δq, %	0.189	0.461	0.901	1.448	0.732	0.511
Freundlich	K_F, (mg/g)(L/mg)$^{1/n}$	0.006	0.029	0.038	0.002	0.002	0.025
	n	0.820	0.963	0.979	0.572	0.680	0.906
	R^2	0.968	0.983	0.976	0.989	0.998	0.997
	Δq, %	1.576	0.810	0.758	3.103	1.347	0.511
Temkin	A, L/mg	16.43	19.42	1.519	18.65	21.72	25.25
	B, kJ/mol	0.005	0.006	0.008	0.004	0.005	0.006
	R^2	0.968	0.971	0.522	0.910	0.925	0.961
	Δq, %	7.463	1.040	13.58	5.481	5.978	3.799
Sips	K_s, L/mg	0.0018	0.0014	0.0014	0.0013	0.001	0.001
	q_m, mg/g	34.63	57.32	67.21	45.64	164.6	192.8
	n_s	3.075	1.822	1.565	3.151	1.723	1.316
	R^2	0.997	0.993	0.9888	0.999	0.998	0.998
	Δq, %	8.819	27.23	3.0635	21.10	138.9	129.6
Redlich–Peterson (RP)	K_R, L/g	0.029	0.061	0.0495	5.269	7.347	7.838
	a_R, (L/m)β	0.051	0.016	0.0054	191.0	202.0	159.5
	β	1.85×10^{-17}	1.05×10^{-17}	1.8×10^{-17}	7.9×10^{-17}	5.9×10^{-17}	2.1×10^{-17}
	R^2	0.955	0.983	0.9861	0.921	0.955	0.925
	Δq, %	1.157	2.306	10.364	5.132	4.109	5.332
Dubinin–Radushkevich (DR)	q_m, mg/g	34.63	42.74	45.831	46.64	52.25	57.99
	k_{DR}, mol^2/J^2	0.023	0.031	0.0383	0.035	0.053	0.068
	E, kJ/mol	4.625	4.036	3.613	3.801	2.920	2.704
	R^2	0.987	0.938	0.894	0.993	0.963	0.921
	Δq, %	12.88	8.917	6.276	22.57	13.93	7.749

The treatment with methanol allows a higher removal Cr(III) around 20% compared to the treatment with water. The values of energy necessary to transfer Cr(III) ions to the surface of the biosorbent [24,32,40] decrease with pH rise, indicating that at lower energy, Cr(III) adsorption increase regardless of the pretreatment and the pH of the medium. When $E > 8$ kJ/mol, the Dubinin–Radushkevich model indicates Cr(III) physical processes [3,24,40]. Also, it is essential to highlight that the adsorption process was spontaneous $\Delta G < 0$ [3,24,36,40].

3.3. Effect of contact time

Fig. 5 shows the contact time at the different pHs for WGP and MGP. A rapid adsorption Cr(III) adsorption was observed regardless of the pretreatment until physicochemical equilibrium after 3 h after starting the adsorption process, after this time the removal becomes slow until reaching a removal percentage of 50% for the MGP sample with a pH of 2.7 [29,43,47,56–59].

3.4. Kinetics of Cr(III) adsorption

The analysis of the adsorption process of Cr(III) in GP concerning time could be described with the different kinetic models (Tables 4 and 5) by determining its parameters. The deterministic coefficient and the normalized standard deviation showed us that the Elovich, intraparticle diffusion and external diffusion models do not describe the experimental data as behavior indicating that there are no limitations due to mass transfer. Avrami model presented more adequate predictions based Δq% values followed by pseudo-first-order, pseudo-second-order. $n_A < 1$, the adsorption process may have several mechanisms involved. Various authors suggest that this behavior in equilibrium studies indicates chemisorption and physical adsorption Cr(III) adsorption capacity using WGP at 60°C was from 38.22 to 133 mg/g when increasing the pH from 0.93 to 2.74, in the case of MGP it was from 41 to 141, 4 when increasing the pH from 0.94 to 2.74. These results have the same trend shown in the Cr removal equilibrium analysis, the greater

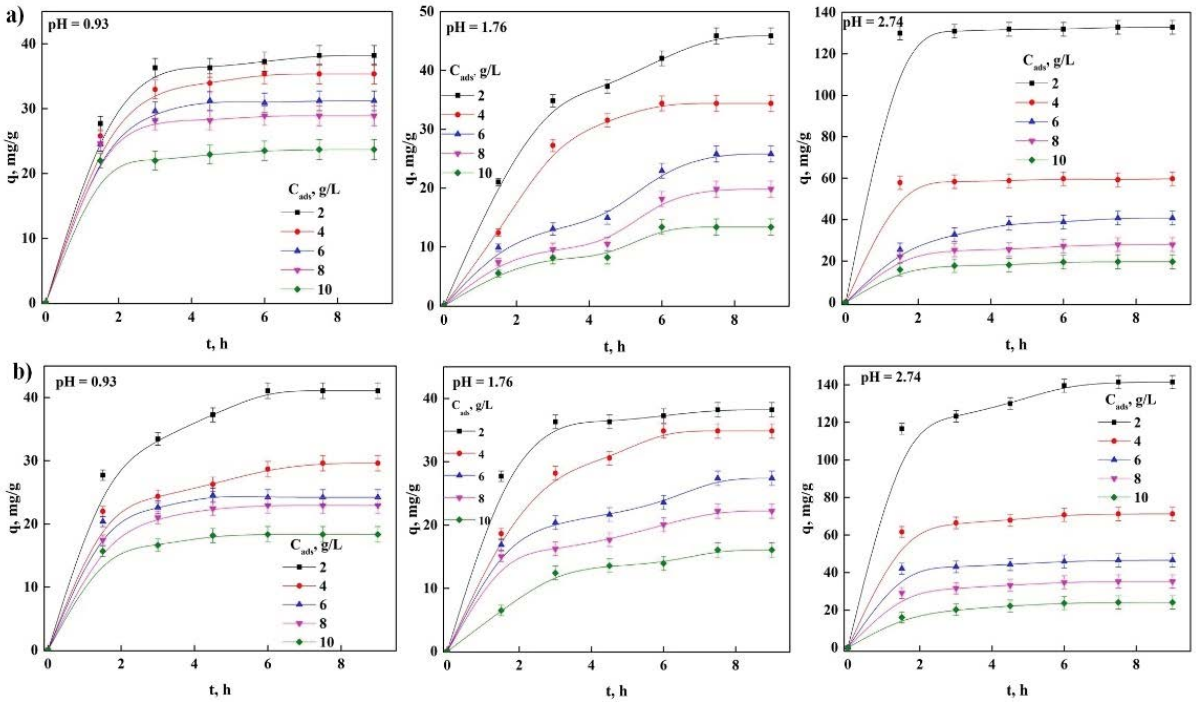

Fig. 5. Adsorption of Cr(III) in function to contact time: (a) WGP and (b) MGP.

Table 4
Non-linear models for Cr(III) removal using WGP at doses 2, 4, 6, 8, and 10 g/L and pH 0.93, 1.76, and 2.74

Model	2 g/L			4 g/L			6 g/L			8 g/L			10 g/L		
	0.93	1.76	2.74	0.93	1.76	2.74	0.93	1.76	2.74	0.93	1.76	2.74	0.93	1.76	2.74
pseudo-first-order															
q_{max}, mg/g	37.9	30.77	136.2	35.29	41.32	59.16	31.2	34.46	40.56	28.76	31.35	27.15	23.21	16.21	19.2
k_1, 1/h	0.895	0.283	2.785	0.876	0.242	2.499	1.0252	0.164	0.615	1.286	0.121	1.075	1.888	0.217	1.098
R^2	0.998	0.981	0.999	0.999	0.952	0.999	0.9998	0.965	0.997	0.995	0.945	0.993	0.996	0.950	0.995
Δq, %	0.331	13.44	1.028	0.079	8.203	0.382	0.017	13.71	0.208	0.203	23.75	1.166	0.838	17.80	1.002
Pseudo-second-order															
q_{max}, mg/g	41.71	68.72	133.1	38.66	59.8	59.86	33.66	51.76	47.73	30.29	30.33	29.37	23.95	23.15	20.72
k_2, 1/h	0.036	0.004	0.192	0.037	0.003	0.285	0.059	0.002	0.017	0.104	0.002	0.069	0.260	0.0073	0.101
R^2	0.994	0.982	1.000	0.997	0.945	0.999	0.997	0.966	0.998	0.999	0.944	0.998	0.998	0.951	0.998
Δq, %	3.771	20.34	0.088	3.818	30.15	6.972	3.201	41.10	6.972	1.958	21.63	2.077	0.437	29.86	2.150
Elovich															
α, mg/g·h	825.5	34.79	1000	669.6	21.37	2812	369.4	14.63	117.4	1075	10.28	2185	1228	3.609	1917
β, g/mg	0.188	0.064	0.061	0.192	0.070	0.378	0.279	0.101	0.113	0.439	0.124	0.308	0.870	0.200	0.448
R^2	0.988	0.979	0.967	0.990	0.945	0.948	0.992	0.951	0.994	0.996	0.917	0.999	0.999	0.944	0.999
Δq, %	6.826	9.2332	26.97	22.00	3.048	18.78	24.45	5.758	18.78	18.55	5.758	20.90	16.54	8.322	16.64
Avrami															
q_{max}, mg/g	38.02	50.766	132.1	35.34	36.32	59.66	31.22	24.46	40.66	28.86	20.35	27.75	23.27	13.21	19.73
k_A, 1/h	0.774	0.295	2.744	0.945	0.404	2.588	1.041	0.322	6.746	1.286	0.261	1.103	1.388	0.250	1.106
n	0.961	0.958	1.000	0.927	0.599	0.966	0.985	0.510	0.825	0.994	0.464	0.978	1.000	0.866	0.992
R^2	0.999	0.989	0.999	0.999	0.982	0.999	0.999	0.985	0.997	0.999	0.984	0.993	0.996	0.990	0.993
Δq, %	0.128	4.358	0.060	0.018	2.279	0.040	0.013	2.120	0.107	0.058	1.098	0.290	0.0251	0.540	0.093

Table 5
Non-linear models for Cr(III) removal using MGP at doses 2, 4, 6, 8, and 10 g/L and pH 0.93, 1.76, and 2.74

Model	2 g/L			4 g/L			6 g/L			8 g/L			10 g/L		
	0.93	1.76	2.74	0.93	1.76	2.74	0.93	1.76	2.74	0.93	1.76	2.74	0.93	1.76	2.74
Pseudo-first-order															
q_{max}, mg/g	40.75	60.89	136.8	28.58	35.63	69.85	24.15	26.26	45.36	22.86	21.03	32.79	18.12	16.52	23.88
k_1, 1/h	0.674	0.449	1.161	0.847	0.498	1.374	1.195	0.558	1.676	0.932	0.635	0.901	1.253	0.386	0.693
R^2	0.992	0.964	0.988	0.985	0.997	0.997	0.998	0.966	0.995	0.999	0.956	0.987	0.995	0.986	0.997
Δq, %	0.334	0.175	1.329	1.434	0.883	1.339	0.094	1.686	1.002	0.128	2.180	1.814	0.480	1.189	0.354
Pseudo-second-order															
q_{max}, mg/g	46.73	73.97	147.3	31.88	43.349	73.55	25.64	30.86	47.17	25.01	24.35	36.37	19.23	21.37	27.32
k_2, 1/h	0.020	0.007	0.015	0.041	0.013	0.045	0.104	0.022	0.102	0.065	0.035	0.239	0.145	0.017	0.035
R^2	0.997	0.979	0.996	0.995	0.994	0.999	0.998	0.983	0.998	0.998	0.977	0.997	0.998	0.983	0.996
Δq, %	5.608	8.557	1.708	3.114	12.26	1.356	2.416	5.186	0.587	3.682	3.923	2.340	1.968	13.52	5.479
Elovich															
α, mg/g·h	173.9	91.520	1742	325.1	53.57	2487	1988	59.76	5798	74.84	72.69	514.6	15397	14.53	109.9
β, g/mg	0.124	0.065	0.065	0.215	0.107	0.179	0.454	0.166	0.359	0.323	0.228	0.198	0.605	0.1938	0.215
R^2	0.996	0.985	0.998	0.998	0.988	0.999	0.995	0.990	0.999	0.994	0.987	0.993	0.998	0.981	0.996
Δq, %	20.13	16.89	28.98	27.55	18.85	14.17	17.31	17.66	8.999	23.05	17.25	4.152	12.41	9.365	18.11
Avrami															
q_{max}, mg/g	40.95	60.98	139	28.98	34.63	70.85	24.18	27.09	45.46	22.96	22.03	33.79	18.28	16.05	23.98
k_A, 1/h	0.778	0.492	0.800	0.945	0.651	1.374	1.200	0.690	1.676	0.961	0.756	0.935	1.253	0.550	0.789
n	0.868	0.913	1.173	0.899	0.764	0.999	0.996	0.809	1.000	0.970	0.841	0.964	1.000	0.741	0.878
R^2	0.992	0.984	0.989	0.988	0.997	0.999	0.998	0.960	0.999	0.999	0.986	0.997	0.999	0.986	0.996
Δq, %	0.133	0.112	0.463	0.880	0.288	0.192	0.042	0.454	0.794	0.055	0.343	0.725	0.142	0.001	0.1734

adsorption capacity is with MGP compared to WGP, which indicates that treatment influences directly the adsorption capacity of the materials and not on the nature of the absorption process, since both biomaterials have an endothermic, spontaneous character and have the presence of chemical and physical mechanisms for the reaction of Cr(III).

The values of the adsorption capacity of Cr(III) with different materials reported in the literature are shown in Table 6 where it was possible to notice that there are differences about the best model that fits the kinetic data of the Cr(III) adsorption where it is mentioned that the removal of Cr involves two active sites for each ion that the majority of studies where this result is obtained are biocarbon from different sources, peel of different fruits treated with water, or chemically treated materials. In our case, even though the Avrami model was considered the best model, this does not limit the use of one or two active sites for the adsorption of Cr(III) the adsorption of Cr(III) allows us to infer that the surface of the biomaterial is heterogeneous and therefore has more than one adsorption mechanism. It can also be mentioned that there is better adsorption with the MGP compared to several biosorbents except those that are chemically synthesized and biochar.

3.5. Study of the surface biosorbents with XRD and ATR-FTIR

Fig. 6 shows the ATR-FTIR spectra of GP with both treatments and at different pH in the Cr(III) adsorption process. The following bands are shown in both spectra: between 3,300–3,000 cm^{-1} it corresponds to the stretching vibration of the O–H group of lignin, cellulose and pectin. The band between 1,740–1,730 cm^{-1} is attributed to the stretching vibration of the C=O bond of the carboxylic groups (–COOH and $–COOCH_3$). The peak found at 1,635–1,615 cm^{-1} are related to the asymmetric stretching vibration of the ionic carboxylic groups while peaks between 1,356–1,334 cm^{-1} are attributed to the symmetric stretching vibration of –COO– pectin. The C–O group belonging to the lignin structure has a stretching vibration between 1,030–1,015 cm^{-1} [3,6,22,25,59]. These characteristic bands of GP that are in both biomaterials present changes in frequency indicating that treatment directly influences the number of groups that are on the surface since several compounds such as flavonoids, and polyphenols are extracted in greater quantity with methanol in compression with water, which causes a significant modification in the presence of different links belonging to these compounds. In addition, some only bands only appear in some pretreated biosorption: at 2,850 cm^{-1} attributed to the asymmetric stretching vibration of the CH groups in MGP and 1,135 cm^{-1} corresponding to the C–O stretching vibration in the lignin structure in WGP [3,6,22,25,59] which indicates that there are different groups and the number of them that act in the removal process of Cr(III) ions.

On the other hand, bands were found that regardless of the treatment do not change in frequency; these are 478; 1,242 and 645 cm^{-1} corresponding to the symmetric stretching

Table 6
Adsorption capacity of Cr(III) of different biosorbents

Adsorbents	*q*, mg/g	Kinetic	References
Lignin biochar	378.3		[26]
Pineapple peel biochar	21.7		[20]
Biochar from coconut shells and olive stone	0.0018		[43]
Pineapple peel biochar	4		[19]
Manure biochar	34.9–38.4		[48]
Biochar from tomato stems and leaves	62.2–169.5		[21]
Cladophora glomerata	37.2		[23]
Ceratophyllum demersum	163.9	Pseudo-second-order	
Jackfruit shell	12.03		[13]
Corn husk washed with H_2O	47.8		[14]
Wheat husk washed with H_2O	43.6		
Citric acid modified cellulose	88.8		[4]
Mejdool and sagae leaf powder	162–194		[57]
Cotton waste	217.1		[55]
Mine waste	86.2		[52]
Human hair waste	15.4		[46]
Marble dust	188.1–106.6	Avrami	[28]
Orange peel treated with methanol	55	Elovich	[24]
Grapefruit peel washed with H_2O	6.75	Pseudo-second-order	[3]
MGP	141.1	Avrami	This work
WGP	133		

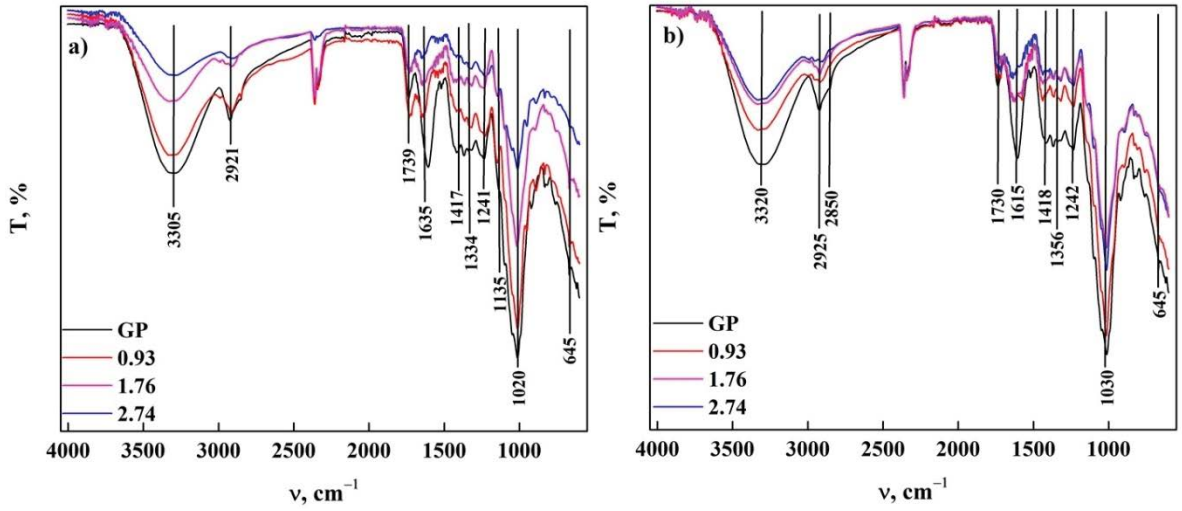

Fig. 6. ATR-FTIR spectra of GP used in Cr(III) adsorption: (a) treatment with water and b) treatment with methanol.

vibration of the carboxylate carbonyl ν(–CO) and inflection vibration of aromatic compounds, respectively. Furthermore, after Cr(III) adsorption, the intensity of several bands decreases. Also, as pH rise, the intensity of bands decreases, indicating a direct relationship with the pH. This result is particularly intense when GP is treated with methanol indicating that the functional groups act as captors of the surface Cr(III) ions. The phenomena mentioned above are reported by Dinh et al. [3], highlighting the possible interactions of pectin from grapefruit peel, that is, there is more than one Cr(III) removal mechanism: electrostatic forces and n–π interactions. Also, Patiño-Saldivar et al. [24] using orange peel as a biosorbent mentions that there is more than one Cr(III) adsorption mechanism where functional groups and physical processes on the surface intervene. These reports indicate that it is crucial to treat GP to eliminate those compounds that can interfere with the biosorption process, including essential oils that exist on the surface, which reduce their presence by pretreating the shell with water and methanol. The hydroxyl and carboxylic groups that participate significantly

in the adsorption of Cr(III) on the surface of biosorbents are those found in lignin, pectin, and flavonoids.

Fig. 7 shows the diffractograms of GP treated with water and metal after adsorption of Cr(III) at a pH of 2.7. The two peaks observed at 15.3° and around 21° in both biosorbents indicate highly crystalline cellulose material [23]. Cr(III) ions could be observed in MGP at a peak around 38.4° which has been reported in other studies using similar biosorbents [31]. A significant change in the lattice parameter (a_0) is observed with the presence of Cr for WGP, decreasing from 7.07 to 7.4 Å. For MGP a_0 decreases from 7.08 to 6.98 Å. These results indicate that Cr ions are within the GP crystal lattice, which may be due to the substitution of the Ca ions whose ionic radius is 1.22 Å while that of Cr is 0.66 Å, suggesting that a small part of the Cr ions are introduced into the GP in the adsorption process [32].

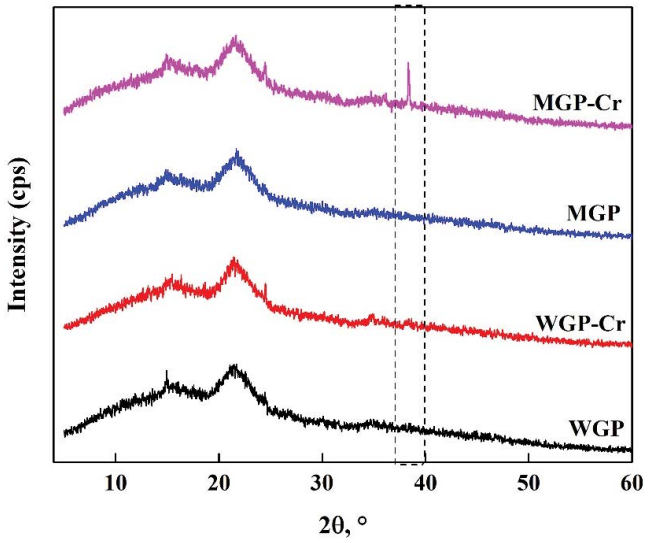

Fig. 7. XRD of GP was used in Cr(III) adsorption at pH 2.7 with different treatments.

3.6. Elemental analysis (EDS) and morphology (SEM) of GP

Through scanning electron microscopy (SEM) the analysis of the GP surface with the two treatments was carried out (Fig. 7). It was possible to observe that in WGP and MGP (Fig. 7a and b) have a thick surface texture and rough cavities characteristic of a mesoporous structure that allows the capture of Cr(III) ions (Fig. 7c and d)

Table 7
Elemental analysis of GP treated with methanol and water

Biosorbents	% wt					
	C	O	Ca	Mg	K	Cr
WGP	56.54	36.86	3.91	0.05	0.05	0.0
MGP	44.37	48.45	6.00	0.05	0.04	0.0
WGP-Cr	47.52	48.36	3.05	0.0	0.0	0.19
MGP-Cr	49.85	48.96	0.71	0.0	0.03	0.36

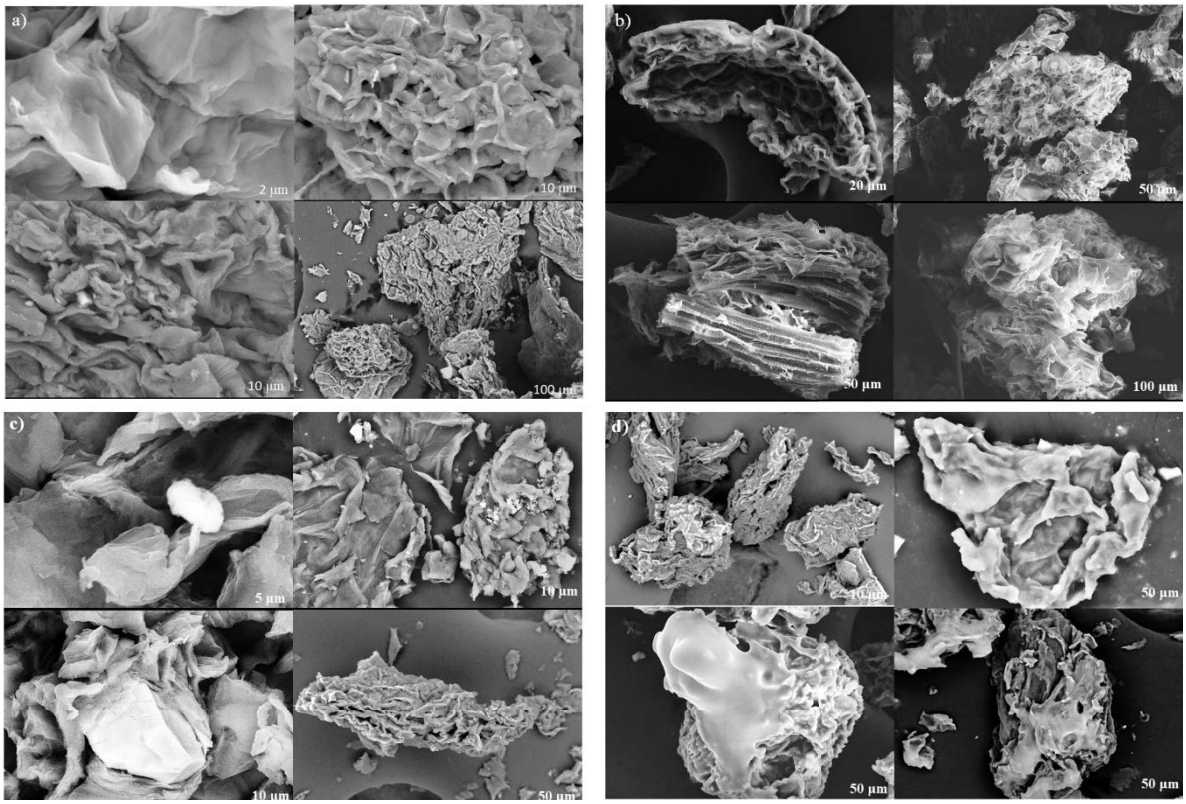

Fig. 8. Micrograph of GP treated before and after Cr adsorption: (a) WGP, (b) MGP, (c) WGP-Cr and (d) MGP-Cr.

[3,4,6,25,59]. The elemental analysis of the grapefruit peel treated with methanol and water was examined using of EDS, obtaining the results shown in Table 7. It was possible to notice a significant change in the C/O ratio of both biosorbents, it a value of 1.53 and 0.92 for WTOP and MGP, respectively. Although the concentration of Mg and K ions remains practically constant and in the case of Ca ions there is a relation 1.53 times higher in GP treated with methanol than GP treated with water [3,4,6,25,59].

When the samples were analyzed after the biosorption of Cr(III). MGP presented a 1.89 times greater amount of Cr(III) than WGP. This result is directly related to the Ca decrease in both samples (22% and 88.2% for WGP and MGP, respectively), confirming that there is an ion exchange between Ca and Cr [31], which was found with the GP lattice parameter when modified significantly due to this substitution. These results also confirm the hypothesis is more than one adsorption mechanism in this process with this biosorbent, these being: (i) ion exchange between Ca and Cr, (ii) complexation of Cr(III) with functional groups present on the surface, and (iii) electrostatic forces.

4. Conclusion

In the present work, the biosorption of Cr(III) was analyzed using grapefruit peel (*Citrus aurantium*) and the mechanisms that rule this removal metal from the solution. It was found that the parameters studied such as contact time, pH, initial metal concentration and adsorbent doses play a crucial role in the Cr ion removal process. Likewise, equilibrium biosorption studies show a favorable process on a heterogeneous surface with a predominant chemical mechanism (Freundlich model), with the removal of 85.75% and 96.6% Cr(III) for WGP and MGP, respectively. The kinetic study of Cr(III) adsorption using GP indicates two stages, the first is a rapid diffusion 3 h after biosorption begins and after this step, the equilibrium phase is reached achieving a maximum adsorption capacity of 133 and 141.4 mg/g for WGP and MGP, respectively. The elimination of this metal from the solution is of chemical origin according to several shreds of evidence (Avrami model); the participation of the different functional groups that exist on the surface of the biosorbents and part of Cr(III) ions are adsorbed within the GP crystal lattice causing an ion exchange with the Ca ions in the lattice structure. Finally, our findings demonstrate that GP is a cheap biosorbent, friendly to the environment and easy to treat to obtain an adsorption capacity comparable to commercial adsorbents for removing of Cr(III) from effluents.

Acknowledgments

The researchers want to thank UPIIG-IPN for the infrastructure provided, as well as the financing through the SIP project: 20210475 and Laboratorio de Investigación y Caracterización de Minerales y Materiales (LICAMM UG).

Conflict of interest

The authors have no conflict of interest to declare.

Symbols

A	—	Temkin isotherm equilibrium binding constant, L/mg
a_R	—	Redlich–Peterson model constant, L/mg
a_0	—	Lattice parameter
B	—	Temkin isotherm constant, kJ/mol
C_o	—	Cr(III) initial concentration, mg/L
C_e	—	Cr(III) concentration in the liquid phase, mg/L
E	—	Energy required to remove a dye molecule from the solution, kJ/mol
k_1	—	Speed constant of the pseudo-first-order model, 1/t
k_2	—	Speed constant of the pseudo-second-order model, g s/mg
k_{DR}	—	Speed constant, $(mol/J)^2$
k_A	—	Kinetic constant, 1/t
k_{ID}	—	Speed constant of the intraparticle diffusion model, mg/g·h
k_{ext}	—	Speed constant of the model external diffusion, 1/h
K_F	—	Freundlich model constant related to the adsorption capacity, $(mg/g)(L/mg)^{1/n}$
K_L	—	Langmuir model constant, mg/L
K_R	—	Redlich–Peterson model isotherm constant, L/g
K_s	—	Sips constant related to energy adsorption, L/mg
m	—	Mass of nDCPD, g
N	—	Number of data
n_A	—	Avrami exponent
n_s	—	Sips model dimensionless parameter
q_{cal}	—	Calculated value of Cr(III) ions adsorbed in equilibrium, mg/g
n_{RP}	—	Redlich–Peterson model exponent
q_e	—	Concentration of Cr(III) in equilibrium with the solid phase, mg/g
q_{exp}	—	Experimental value of Cr(III) ions adsorbed in equilibrium, mg/g
q_m	—	Maximum Cr(III) concentration adsorbed by the adsorbent mass, mg/g
Δq	—	Normalized coefficient of determination
R	—	Ideal gases constant, kJ/mol·K
R_L	—	Separation factor, dimensionless parameter
T	—	Absolute temperature, K
V	—	Solution volume, L
ΔG	—	Gibbs free energy, kJ/mol
$\%R_{Cr}$	—	Cr(III) removal percentage
$1/n$	—	Adsorption reaction energy
α	—	Initial rate of adsorption, mg/g·h
β	—	Constant of the Elovich model related to the surface area covered and the activation energy by chemisorption, mg/g
ξ	—	Parameter of the Dubinin–Radushkevich model, $\varepsilon = RT\ln(1 + 1/C_e)$, J/mol

References

[1] L. Joseph, Y. Yoon, B.M. Jun, J.R.V. Flora, C.M. Park, Y. Yoon, Removal of heavy metals from water sources in the developing world using low-cost materials: a review, Chemosphere, 229 (2019) 142–159.

[2] E. Pertile, V. Vaclavik, T. Dvorsky, S. Heviankova, The removal of residual concentration of hazardous metals in wastewater from a neutralization station using biosorbent—a case study company Gutra, Czech Republic, Int. J. Environ. Res. Public Health, 17 (2020) 7225–7237.
[3] V.-P. Dinh, T.-D. Huynh, H.M. Le, V.D. Nguyen, V.-A. Dao, N.Q. Hung, L.A. Tuyen, S. Lee, J. Yi, T.D. Nguyen, L.V. Tan, Insight into the adsorption mechanisms of methylene blue and chromium(III) from aqueous solution onto pomelo fruit peel, RSC Adv., 9 (2019) 25847–25860.
[4] S. Batool, H. Ullah, M. Idrees, M.I. Al-Wabel, M. Ahmad, K. Hin, L. Cui, Q. Hussain, Sorption of Cr(III) from aqueous media via naturally functionalized microporous biochar: mechanistic study, Microchem. J., 144 (2019) 242–253.
[5] X. Liu, Y. Wan, P Liu, Y. Fu, W. Zou, A novel activated carbon prepared from grapefruit peel and its application in removal of phenolic compounds, Water Sci. Technol., 77 (2018) 2517–2527.
[6] H. Wang, J. Xu, X. Liu, L. Sheng, Preparation of straw activated carbon and its application in wastewater treatment: a review, J. Cleaner Prod., 283 (2021) 124671, doi: 10.1016/j.jclepro.2020.124671.
[7] M. Torab-Mostaedi, M. Asadollahzadeh, A. Hemmati, A. Khosravi, Biosorption of lanthanum and cerium from aqueous solutions by grapefruit peel: equilibrium, kinetic and thermodynamic studies, Res. Chem. Intermed., 41 (2015) 559–573.
[8] S. Afroze, T. Kanti Sen, A review on heavy metal ions and dye adsorption from water by agricultural solid waste adsorbents, Water Air Soil Pollut., 229 (2018) 225, doi: 10.1007/s11270-018-3869-z.
[9] L. Pietrelli, I. Silvestro, I. Francolini, A. Piozzi, M. Sighicelli, M. Vocciante, Chromium(III) removal from wastewater by chitosan flakes, Appl. Sci., 10 (2020) 1925, doi: 10.3390/app10061925.
[10] B. Kaźmierczak, J. Molenda, M. Swat, The adsorption of chromium(III) ions from water solutions on biocarbons obtained from plant waste, Environ. Technol. Innovation, 23 (2021) 101737, doi: 10.1016/j.eti.2021.101737.
[11] M.A. Hashem, M. Hasan, M.A. Momen, S. Payel, M.S. Nur-A-Tomal, Water hyacinth biochar for trivalent chromium adsorption from tannery wastewater, Environ. Sustainability Indic., 5 (2020) 100022, doi: 10.1016/j.indic.2020.100022.
[12] S. Wierzba, A. Kłos, Heavy metal sorption in biosorbents – using spent grain from the brewing industry, J. Cleaner Prod., 225 (2019) 112–120.
[13] S.H. Ranasinghe, A.N. Navaratne, N. Priyantha, Enhancement of adsorption characteristics of Cr(III) and Ni(II) by surface modification of jackfruit peel biosorbent, J. Environ. Chem. Eng., 6 (2018) 5670–5682.
[14] Y. Chen, Q. Chen, H. Zhao, J. Dang, R. Jin, W. Zhao, Y. Li, Wheat straws and corn straws as adsorbents for the removal of Cr(VI) and Cr(III) from Aqueous solution: kinetics, isotherm, and mechanism, ACS Omega, 5 (2020) 6003–6009.
[15] M.D. Islam, A. Rahamad, M.M. Mahdi, D. Malik, Removal of Cr(III) and other pollutants from tannery wastewater by *Moringa stenopetela* seed, IOP Conf. Ser.: Earth Environ. Sci., 644 (2021) 012025, doi: 10.1088/1755-1315/644/1/012025.
[16] E. Rosales, J. Meijide, T. Tavares, M. Pazos, M.A. Sanromán, Grapefruit peelings as a promising biosorbent for the removal of leather dyes and hexavalent chromium, Process Saf. Environ. Prot., 101 (2016) 61–71.
[17] R. Wang, M. Zhong, W. Li, Y. Chen, Z. Tan, X. Li, J. Zhang, Isothermal and kinetic studies of biosorption of low concentration Cr(III) from aqueous solution by 4 microbial biosorbents, Pol. J. Environ. Stud., 31 (2022) 1363–1376.
[18] J.S. Bădescu, D. Bulgariu, I. Ahmad, L. Bulgariu, Valorisation possibilities of exhasted biosorbents loaded with metal ions – a review, J. Environ. Manage., 224 (2018) 288–297.
[19] E. Sforza, P. Kumkum, E. Barbera, S. Kumar, Bioremediation of industrial effluents: how a biochar pretreatment may increase the microalgal growth in tannery wastewater, J. Water Process Eng., 37 (2020) 101431, doi: 10.1016/j.jwpe.2020.101431.
[20] A.L. Arim, G. Guzzo, M.J. Quina, L.M. Gando-Ferreira, Single and binary sorption of Cr(III) and Ni(II) onto modified pine bark, Environ. Sci. Pollut. Res., 25 (2020) 28039–28049.
[21] J. Mokrzycki, I. Michalak, P. Rutkowski, Biochars obtained from freshwater biomass—green macroalga and hornwort as Cr(III) ions sorbents, Biomass Convers. Biorefin., 11 (2021) 301–313.
[22] J. Bayo, G. Esteban, J. Castillo, The use of native and protonated grapefruit biomass (*Citrus paradisi L.*) for cadmium(II) biosorption: equilibrium and kinetic modelling, Environ. Technol., 33 (2012) 761–772.
[23] J. Mokrzycki, I. Michalak, P. Rutkowski, Tomato green waste biochars as sustainable trivalent chromium sorbents, Environ. Sci. Pollut. Res., 28 (2021) 24245–24255.
[24] L. Patiño-Saldivar, J.A. Hernández, A. Ardila, M. Salazar-Hernández, A. Talavera, R. Hernández-Soto, Cr(III) removal capacity in aqueous solution in relation to the functional groups present in the orange peel (*Citrus sinensis*), Appl. Sci., 11 (2021) 6346, doi: 10.3390/app11146346.
[25] M. Torab-Mostaedi, M. Asadollahzadeh, A. Hemmati, A. Khosravi, Equilibrium, kinetic, and thermodynamic studies for biosorption of cadmium and nickel on grapefruit peel, J. Taiwan Inst. Chem. Eng., 44 (2013) 295–302.
[26] J. Xue, J. Cai, A. Aihemaiti, Y. Li, Removal of Cr(III) from aqueous solutions by carbon lignin-based composite, Sep. Sci. Technol., 57 (2021) 523–531.
[27] I. Anastopoulos, G. Kyzas, Agricultural peels for dye adsorption: a review of recent literature, J. Mol. Liq., 200 (2014) 381–389.
[28] T. Guimarães, L.D. Paquini, F.R. Lyrio Ferraz, L.P.R. Profeti, D. Profeti, Efficient removal of Cu(II) and Cr(III) contaminants from aqueous solutions using marble waste powder, J. Environ. Chem. Eng., 8 (2020) 103972, doi: 10.1016/j.jece.2020.103972.
[29] A.S. Daniel, E. Zahir, I. Hussain, S. Naz, M.A. Asghar, Citric acid modified cellulose: a cost-effective adsorbent for the immobilization of Cr(III) ions from the aqueous phase, Energy Sources, Part A, (2020) 1–13, doi: 10.1080/15567036.2020.1773963.
[30] M.E. Jiménez-Castañeda, P.E. Escamilla-García, Chromium removal from water using modified organic materials: a review, Water Qual. Res. J., 55 (2020) 221–233.
[31] A.F. Moreno-García, R. Hernández-Altamirano, E.E. Neri-Torres, Y.V. Mena-Cervantes, M. García-Solares, G. Pineda-Flores, R. Luna-Sánchez, J. Vazquez-Arenas, J.A. Suastes-Rivas, Sustainable biorefinery associated with wastewater treatment of Cr(III) using a native microalgae consortium, Fuel, 290 (2021) 119040, doi: 10.1016/j.fuel.2020.119040.
[32] J.A. Hernandez-Maldonado, F.A. Torres-Garcia, M.M. Salazar-Hernandez, R. Hernandez-Soto, Removal of chromium from contaminated liquid effluents using natural brushite obtained from bovine bone, Desal. Water Treat., 95 (2017) 262–273.
[33] A.G. Varghese, S.A. Paul, M.S. Latha, Remediation of heavy metals and dyes from wastewater using cellulose-based adsorbents, Environ. Chem. Lett., 17 (2019) 867–877.
[34] B.E. López-Muñoz, R. Rivera-Robles, J.L. Iturbe-García, M.T. Olguín-Gutiérrez, Adsorption of basic chromium sulfate used in the tannery industries by calcined hydrotalcite, J. Mex. Chem. Soc., 55 (2011) 137–141.
[35] A. Dasque, M. Gressier, P.-L. Taberna, M.-J. Menu, Characterization of chromium(III)-glycine complexes in an acidic medium by UV-visible spectrophotometry and capillary electrophoresis, Results Chem., 3 (2021) 100207, doi: 10.1016/j.rechem.2021.100207.
[36] L. Nemeş, L. Bulgariu, Optimization of process parameters for heavy metals biosorption onto mustard waste biomass, Open Chem., 14 (2016) 175–187.
[37] I. Acosta-Rodríguez, A. Rodríguez-Pérez, N.C. Pacheco-Castillo, E. Enríquez-Domínguez, J.F. Cárdenas-González, V.-M. Martínez-Juárez, V.-M. Removal of cobalt(II) from waters contaminated by the biomass of *Eichhornia crassipes*, Water, 13 (2021) 1725–1736.
[38] R. Sudha, K. Srinivasan, P. Premkumar, Removal of nickel(II) from aqueous solution using *Citrus limettioides* peel and seed carbon, Ecotoxicol. Environ. Saf., 117 (2015) 115–123.

[39] G.Z. Kyzas, D.N. Bikiaris, A.C. Mitropoulos, Chitosan adsorbents for dye removal: a review, Polym. Int., 66 (2017) 1800–1811.
[40] E. Joaquín-Medina, L. Patiño-Saldivar, A.N. Ardilas-Arias, M. Salazar-Hernández, Hernández, Bioadsorption of methyl orange and methylene blue contained in water using as bioadsorbent Natural Brushite (nDCPD), Tecnología y Ciencias del Agua, 12 (2021) 304–347.
[41] X.S. Wang, Y. Zhou, Y. Jiang, C. Sun, The removal of basic dyes from aqueous solutions using agricultural by-products, J. Hazard. Mater., 157 (2008) 374–385.
[42] A. El-Hamidi, R. Mulongo-Masamba, M. Khachani, M. Halim, S. Arsalane, Kinetics modeling in liquid phase sorption of copper ions on brushite di-calcium phosphate di-hydrate $CaHPO_4{\cdot}2H_2O$ (DCPD), Desal. Water Treat., 56 (2014) 779–791.
[43] W. Zhang, J. Song, Q. He, H. Wang, W. Lyu, H. Feng, W. Xiong, W. Guo, J. Wu, L. Chen, Novel pectin based composite hydrogel derived from grapefruit peel for enhanced Cu(II) removal, J. Hazard. Mater., 384 (2019) 121445, doi: 10.1016/j.jhazmat.2019.121445.
[44] B. Samiley, M.R. Dargahi, Kinetics and thermodynamics of adsorption of Congo red on cellulose, Cent. Eur. J. Chem., 8 (2010) 906–912.
[45] A.A.A. Bakar, N.F.A. Razak, N.A. Akbar, N.M. Daud, K.A.M. Ali, Removal of Cr(III) from industrial wastewater using coconut shell carbon and limestone as adsorbent, IOP Conf. Ser.: Earth Environ. Sci., 646 (2021) 012063, doi: 10.1088/1755-1315/646/1/012063.
[46] R. Kumar, M.A. Laskar, I.F. Hewaidy, M.A. Barakat, Modified adsorbents for removal of heavy metals from aqueous environment: a review, Earth Syst. Environ., 3 (2019) 83–93.
[47] S. Tamjidi, A. Ameri, A review of the application of sea material shells as low cost and effective bio-adsorbent for removal of heavy metals from wastewater, Environ. Sci. Pollut. Res., 27 (2020) 31105–31119.
[48] H. Zhang, F. Carrillo-Navarrete, M. López-Mesas, C. Palet, Use of chemically treated human hair wastes for the removal of heavy metal ions from water, Water, 12 (2020) 1263, doi: 10.3390/w12051263.
[49] C. Awada, H. Traboulsi, Effect of pH and nanoparticle capping agents on Cr(III) monitoring in water: a kinetic way to control the parameters of ultrasensitive environmental detectors, Micromachines (Basel), 11 (2020) 1045, doi: 10.3390/mi11121045.
[50] Y.P. Zhang, V.S.K. Adi, H.-L. Huang, H.-P. Lin, Z.-H. Huang, Adsorption of metal ions with biochars derived from biomass wastes in a fixed column: adsorption isotherm and process simulation, J. Ind. Eng. Chem., 76 (2019) 240–244.
[51] T. Li, Y. Guan, T. Yang, Y. Yu, G. Xu, Q. Han, G. Luo, J. Du, C. Guo, Trivalent chromium removal from tannery wastewater with low cost bare magnetic Fe_3O_4 nanoparticles, Chem. Eng. Process. Process Intensif., 169 (2021) 108611, doi: 10.1016/j.cep.2021.108611.
[52] A. Oumani, L. Mandi, F. Berrekhis, N. Ouazzani, Removal of Cr^{3+} from tanning effluents by adsorption onto phosphate mine waste: key parameters and mechanisms, J. Hazard. Mater., 378 (2019) 120718, doi: 10.1016/j.jhazmat.2019.05.111.
[53] E. Parameswari, R.P. Premalatha, V. Davamani, P. Kalaiselvi, S.P. Sebastian, K. Suganya, Biosorption of chromium ions through modified *Eichhornia crassipes* biomass form the aqueous medium, J. Environ. Biol., 42 (2021) 62–73.
[54] S. Mihajlović, M. Vukčević, B. Pejić, A.P. Grujić, M. Ristić, Application of waste cotton yarn as adsorbent of heavy metal ions from single and mixed solutions, Environ. Sci. Pollut. Res., 27 (2020) 35769–35781.
[55] S. Zhang, C. Liu, Y. Yuan, M. Fan, D. Zhang, D. Wang, Y. Xu, Selective, highly efficient extraction of Cr(III), Pb(II) and Fe(III) from complex water environment with a tea residue derived porous gel adsorbent, Bioresour. Technol., 311 (2020) 123520, doi: 10.1016/j.biortech.2020.123520.
[56] L.A. Romero-Cano, L.V. González-Gutiérrez, L.A. Baldenegro-Pérez, F. Carrasco-Marín, Grapefruit peels as biosorbent: characterization and use in batch and fixed bed column for Cu(II) uptake from wastewater, J. Chem. Technol. Biotechnol., 92 (2017) 1650–1658.
[57] D. Días, N. Lapa, M. Bernardo, W. Ribeiro, I. Matos, I. Fonseca, F. Pinto, Cr(III) removal from synthetic and industrial wastewaters by using cogasification chars of rice waste streams, Bioresour. Technol., 266 (2018) 139–150.
[58] M. Azam, S.M. Wabaidur, M.R. Khan, S.I. Al-Resayes, M.S. Islam, Removal of chromium(III) and cadmium(II) heavy metal ions from aqueous solutions using treated date seeds: an eco-friendly method, Molecules, 26 (2021) 3718, doi: 10.3390/molecules26123718.
[59] K. Pakshirajan, A.N. Worku, M. Acheampong, H.J. Lubberding, P.N.L. Lens, Cr(III) and Cr(VI) removal from aqueous solutions by cheaply available fruit waste and algal biomass, Appl. Biochem. Biotechnol., 170 (2013) 498–513.